

# A Modified PSO Algorithm for Remote Sensing Image Template Matching

Ru An, Peng Gong, Huilin Wang, Xuezhi Feng, Pengfeng Xiao, Qi Chen, Qing Zhang, Chunye Chen, and Peng Yan

## Abstract

*Image template matching is essential in image analysis and computer vision tasks. Cross-correlation algorithms are often used in practice, but they are sensitive to nonlinear changes in image intensity and random noise, and are computationally expensive. In this paper, we propose a template-matching algorithm based on a modified particle swarm optimization (PSO) procedure with a mutual information (MI) similarity measure. The influence of MI on the performance of template matching, calculated by different histogram bins, is analyzed first. A modified PSO method (CRI-PSO) is then presented. The proposed algorithm is tested with remote sensing imagery from different sensors and for different seasons. Our experimental results indicate that the proposed approach is robust in practical scenarios and outperforms the standard PSO, multi-start PSO, and cross-correlation algorithms in accuracy and efficiency with our test data. The proposed method can be used for position estimation of aircraft, object recognition, and image retrieval.*

## Introduction

Image template matching is a process of determining the presence and location of an input image or an object inside a reference image (Choi *et al.*, 2002). The input image and the reference image may be dissimilar because they may exhibit relative translation, rotation, and different scales or contain additive random noise due to different sensors and image captured at different dates. All these factors make

image matching a challenging task (Brown, 1992; Zitova *et al.*, 2003). Image template matching has been widely used for object recognition, image retrieval, motion tracking, aircraft position estimation, change detection, and multi-image registration (An *et al.*, 2005; Gong *et al.*, 1992; Liu *et al.*, 2006; Oh *et al.*, 2006; Sim *et al.*, 1999a and 1999b). Cross-correlation-based algorithms such as the normalized cross-correlation (NCC), the mean absolute error (MAE), and the mean squares error (MSE) methods are often used in image template matching. These methods do not generally require extensive preprocessing, such as segmentation or feature extraction, but they often have a lower probability of correct matching when the image intensity has nonlinear changes. They are also computationally expensive. Other commonly used methods in template matching are feature-based techniques. These methods often fail when the images to be matched contain few salient features such as points, lines, and regions (Brown, 1992; Zitova *et al.*, 2003).

Position estimation of aircraft through image matching is an important method for autonomous navigation. Because of its benefits of higher self-determination and accuracy, the development of image-based navigation systems has been a hot research topic (Sim *et al.*, 1999a and 1999b; Oh *et al.*, 2006). Various approaches, such as terrain contour matching (TERCOM), inertial navigation systems (INS), and global positioning systems (GPS), have been used for navigation, but they all have some drawbacks. For example, the estimation error by the INS tends to increase as an aircraft goes on flying, the GPS can be disturbed by external signals, and terrain contour matching encounters difficulties in estimating its own position in the plain regions where change in the elevation is small and can be out of control by external signals (Oh *et al.*, 2006). In practice, a hybrid system, such as, INS and image-based navigation system is commonly used. INS usually supplies orientation and altitude information of the aircraft and image-based navigation is used to rectify cumulative error and increase accuracy of INS systems.

In general, navigation systems have been developed under the assumption that an aircraft flies along a predetermined (planned) trajectory. Therefore, it is assumed that the system contains reference images, and it is thus possible to measure the performance of various matching methods (Oh *et al.*, 2006). A matching algorithm suitable for position estimation of aircraft has to meet the requirements of reliability (higher success rate for matching), accuracy

---

Ru An, Qing Zhang, Chunye Chen and Peng Yan are with the Department of Geographical Information Sciences, College of Hydrology and Water Resources, Hohai University, Nanjing 210098, China (anrunj@yahoo.com.cn).

Peng Gong is with the Department of Environmental Science, Policy and Management, University of California at Berkeley, 137 Mulford Hall, Berkeley, CA 94720, and State Key Laboratory of Remote Sensing Science, Institute of Remote Sensing Applications of Chinese Academy of Sciences and Beijing Normal University, Beijing 100101, China.

Huilin Wang, Xuezhi Feng, and Pengfeng Xiao are with the Institute of Geography and Sea Sciences, Nanjing University, Nanjing 210093, China.

Qi Chen is with the Department of Geography, University of Hawai'i at Manoa, 422 Saunders Hall, 2424 Maile Way, Honolulu, HI 96822.

Qing Zhang, Chunye Chen and Peng Yan are with the Department of Geographical Information Sciences, College of Hydrology and Water Resources, Hohai University, Nanjing 210098, China.

---

Photogrammetric Engineering & Remote Sensing  
Vol. 76, No. 4, April 2010, pp. 000–000.

0099-1112/10/7604–0000/\$3.00/0  
© 2010 American Society for Photogrammetry  
and Remote Sensing

(precise location), and real-time implementation. Currently, few approaches can meet all these requirements. It is especially difficult to achieve a high success rate and real-time efficiency at the same time.

A template matching algorithm for absolute position estimation (APE) was introduced based on the Hausdorff distance (HD) (Sim *et al.*, 1999a and 1999b), in which aerial images were used as import images, and SPOT images were used as reference images. An accumulated buffer (AB) matching method was suggested by Oh *et al.* (2006), in which some accumulated buffers, such as those employed in the Hough transform, are used as a set of accumulator cells. AB matching is faster than HD matching, and has performance comparable to that of NCC matching.

From the studies mentioned above, we find that the performance of commonly used matching methods does not satisfy practical applications. The NCC method often exhibits slow matching speed and a low matching rate when the image intensity is nonlinear, while AB matching exhibits a fast speed but a low matching rate. Therefore, a more robust similarity measure and a faster matching strategy are required.

Mutual information (MI) has been considered a suitable similarity measure for template matching in which the images to be matched are dissimilar. It is more flexible and independent of image content (Chen *et al.*, 2003). Since its introduction (Viola and Wells, 1995; Maes *et al.*, 1997), MI has been used widely in many multi-modal medical image registration problems because of its generality and high accuracy (Pluim *et al.*, 2001; Lo, 2003; Xu *et al.*, 2007). The registration of remote sensing images using mutual information has also been studied by Inglada (2002), Johnson *et al.* (2001), Cole-Rhodes *et al.* (2003), Chen *et al.* (2003), and Kern (2007). They found that MI produced consistently sharper peaks at the correct registration position than cross correlation, which is important for accurate registration. They also found that mutual information was more robust against Gaussian noise when working at low signal to noise ratios. MI is also robust against nonlinear intensity relationships between images, such as contrast reversals.

The search strategy optimizes the similarity metric. A fast search strategy is very important in practical applications in order to improve efficiency. Examples include local or global searches, multi-resolution approaches, or other optimization techniques. Particle swarm optimization (PSO) is an evolutionary computation technique. Since its introduction (Kennedy and Eberhart, 1995), it has attracted considerable attention from researchers because of its simplicity in concept, requirement of fewer parameters, and ease of implementation (Eberhart *et al.*, 2004). It has found applications in many areas, such as evolving neural networks, tracking dynamic systems, tackling multi-objective optimization, constraint optimization problems, reactive power, and voltage control and ingredient mix optimization (Eberhart *et al.*, 2004; Hu *et al.*, 2004; Alrashidi *et al.*, 2006). In image processing, Wachowiak *et al.* (2004) adapted particle swarm optimization for 3D-to-3D biomedical image registration. The images to be matched were obtained from different modalities. PSO was used as a search strategy to maximize the similarity metric for registering single slice biomedical images to 3D volumes. Knowledge can be incorporated in the initialization of the PSO. Du *et al.* (2005) applied PSO in search of the maximum threshold for infrared image segmentation. Zahara *et al.* (2005) also used a PSO based hybrid optimization approach to optimize multi-threshold image segmentation. Maitra *et al.* (2007) used a PSO based hybrid cooperative-comprehensive learning algorithm for optimizing multilevel threshold for image segmentation. Yin (2006) applied PSO for point pattern

matching, and the experimental results indicate that the PSO-based method is superior to a genetic algorithm and a simulated annealing algorithm in terms of both effectiveness and efficiency.

The main objective of this research is to improve both the accuracy and efficiency in image matching. The focus is on the search strategy for maximizing the similarity metric (MI) in matching. We propose a modified PSO method (CRI-PSO) that improves the swarm diversity and enlarges the search space. It does not destroy the structure of the current particles, and might have high search accuracy. We empirically show that the CRI-PSO achieves better performance than standard PSO and some PSO variants in template matching. A novel image matching method based on MI and CRI-PSO is suggested for aircraft navigation. Generally, INS can ensure only a small flying parametric error, such as 0.5 degree rotation and less than four percent scale variance between the input image and the reference image, so, in the paper, attention is mainly paid on translation transformation.

The paper is organized as follows. In the next Section, a brief discussion of the similarity metric and the influence of different histogram bin sizes on the matching performance are introduced followed by A description of the adaptation of PSO to template matching, and an improved PSO for template matching. An experiment to test the modified algorithm and compare its performance with several other methods is then presented, and finally, some concluding remarks regarding the proposed method.

## Similarity Metric

Similarity metrics are indicators of how closely the features or intensity values of two images match. They must be robust; that is, they should attain a global maximum at the correct matching position.

### Mutual Information Similarity Metric

Mutual information is a concept developed from information theory. It indicates how much information one random variable tells about another. The MI registration criterion can be thought of as a measure of how well one image explains the other. It is applied to measure the statistical dependence between image intensities of corresponding pixels in both images, which is assumed to be a maximum if the images are correctly aligned geometrically.

Mutual information,  $I(U,V)$ , of two random variables  $U$  and  $V$  can be obtained from Equation 1 (Cover *et al.*, 1991):

$$I(U,V) = H(U) + H(V) - H(U,V) \quad (1)$$

where  $H(U)$  and  $H(V)$  are the entropies of  $U$  and  $V$ , and  $H(U,V)$  is their joint entropy. Considering  $U$  and  $V$  as two images, the MI-based matching criterion states that the images shall be registered when  $I(U,V)$  is maximal. The entropies and joint entropy can be computed from:

$$H(U) = -\sum_n p_U(u) \log p_U(u) \quad (2)$$

$$H(V) = -\sum_n p_V(v) \log p_V(v) \quad (3)$$

$$H(U,V) = -\sum_{n,v} p_{UV}(u,v) \log p_{UV}(u,v) \quad (4)$$

where  $p_U(u)$  and  $p_V(v)$  are the marginal probability mass functions, and  $p_{UV}(u,v)$  is the joint probability mass function. These probability mass functions can be obtained from their histograms and joint histogram, respectively (Viola and Wells, 1995; Maes *et al.*, 1997; Chen *et al.*, 2003).

The size of the overlapping part of the images influences the mutual information measure. A normalized measure of mutual information has been proposed (Studholme *et al.*, 1999), which is less sensitive to changes in overlap:

$$NMI(U, V) = \frac{H(U) + H(V)}{H(U, V)}. \quad (5)$$

In all the following experiments (except specific indication is given), Equation 5 is used to calculate similarity measure value for matching.

#### The Number of Histogram Bins and Mutual Information-based Template Matching

In template matching, the size of the input image is often small (e.g.,  $65 \times 65$ ), so determining how many histogram bins should be used to estimate probability distributions is a problem. If the number of bins is too large (e.g., 256 bins), the statistical power of the probability distribution estimation by mutual information will be reduced due to the small number of data points (e.g., pixels for the image) in a bin (Knops *et al.*, 2006). If the number of bins is too small (e.g., 4 bins), important information might be lost. Moreover, in order to reduce the computational complexity, the number of bins used should be as small as possible. Therefore, it is important to select a reasonable number of histogram bins for MI-based template matching. We achieved this aim with empirical experiment. A histogram with 16 bins produced a more highly successful matching rate than a 256 bins histogram. Here, the success rate of matching refers to the ratio between the numbers of successful trials and total trials. For each test image cropped from the input source image, we assume that its theoretically correct matching position in the reference image (e.g., upper left corner) is known in advance. Here, a successful match means that the matching error is within three pixels. The matching error denotes the difference between the theoretically correct matching position and the actual matching position along the x-axis and\or y-axis, respectively. In Figure 1, the correct matching position of an input image is (10, 99),

whereas its actual matching position is (13, 98). Since its location error is in the allowable range (less than three pixels along the x-axis and\or y-axis), it is accepted as a successful match. Computation time refers to the time used in a matching between the reference image and an input image. Moreover, the reduced number of bins dramatically reduces the runtime for MI-based template matching. This image area in Figure 1 is the Farmland.

In Figure 2, the surface of MI similarity measure using different numbers of histogram bins is shown. We can see in Figure 2a that the MI similarity surface is non-convex and irregular, because the size of the images to be matched is only  $65 \times 65$  pixels. This leads the distribution of each pixel sample to spread when the number of bins is 256. We can also observe that the peak of the MI similarity surface at the correct matching position, which is pre-defined (162, 56), is not salient, and it is not the global optimum. The reduced number of histogram bins makes the peak of the histogram much sharper and more distinctive (Figure 2b), and it appears at the correct matching position when the 16-bin histogram is used. However, when the number of bins is too small, it results in multiple peaks in the similarity surface (shown in Figure 2c). This leads to an increased number of incorrect matches. In Figure 2c, we find that the peak of the MI similarity surface at the correct match position is not salient, and it is not the global optimum. Therefore, it is necessary to select a reasonable number of bins for successful matching.

The success rates of MI-based image matching for different numbers of bins are summarized in Table 1. The test data are shown in Figures 1 and 4. We can see that the success rate is greatest when 16 histogram bins are used, and the number of input images for the trials is 100, respectively.

The computation time using MI-based template matching with 16 histogram bins is relatively low (Table 2). The test data of Table 2 is a Stream image pair. Considering the trade-off between the success rate and computation time, we choose 16 histogram bins as a desirable number of bins for relatively high match rates and low computation cost. For a joint histogram, the number of bins is  $16 \times 16$ .

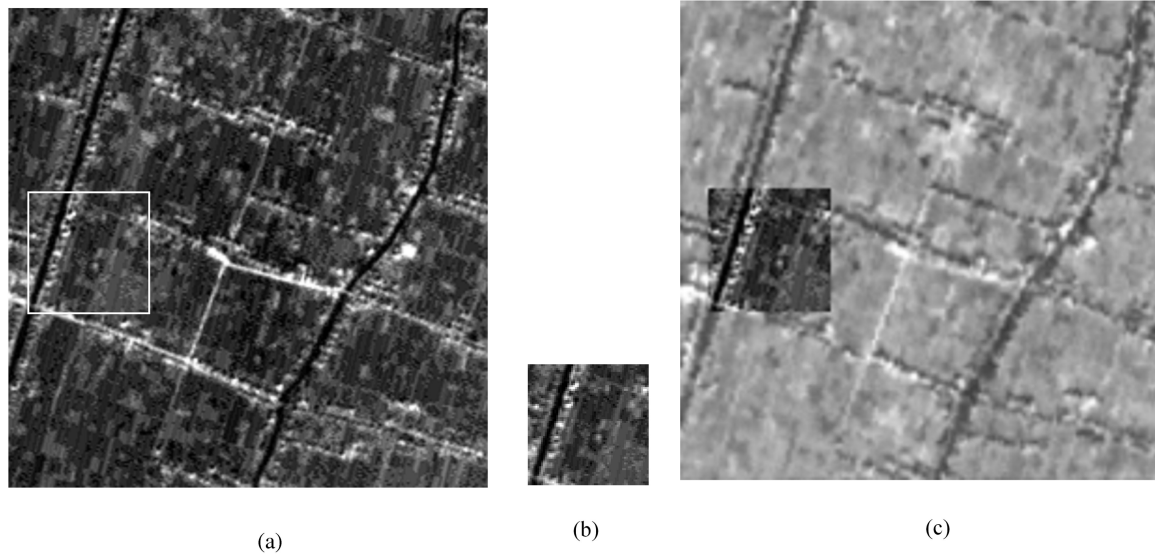


Figure 1. The MI-based template-matching concept: (a) IRS-C source of the template image, (b) a template image cropped from (a), and (c) match result for (b) in (c).

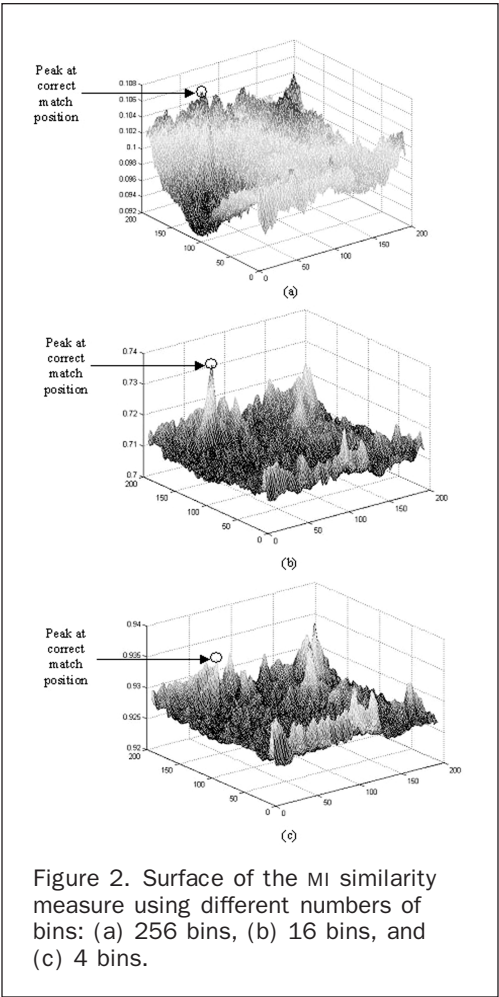


Figure 2. Surface of the MI similarity measure using different numbers of bins: (a) 256 bins, (b) 16 bins, and (c) 4 bins.

TABLE 1. THE SUCCESS RATE OF TEMPLATE MATCHING BASED ON DIFFERENT NUMBERS OF BINs

	Farmland image		Stream image	
	Number of bins	Success rate (%)	Number of bins	Success rate (%)
Normalized mutual information	256	5.5	256	22.0
	128	25.5	128	88.0
	64	47.7	64	99.0
	32	74.4	32	100.0
	16	80.0	16	100.0
	8	72.2	8	98.0
	4	64.3	4	97.0
Mutual information	16	72.1	16	99.0

### Search Strategy

Although using mutual information as a similarity metric is reliable and robust, the computation of the mutual information is complex and the matching speed is slow (Xu *et al.*, 2007) when an exhaustive search method is used (Table 2). Thus, a fast matching search strategy is required in practice. The major advantages of PSO over basic Evolutionary Algorithms (EAs) are that in PSO, each individual benefits from its history, whereas no such mechanism exists in the EAs (Angeline, 1998; Eberhart *et al.*, 1998). The PSO can find

TABLE 2. COMPUTATION TIME REQUIRED WITH DIFFERENT NUMBERS OF BINs IN THE NORMALIZED MUTUAL INFORMATION-BASED TEMPLATE MATCHING WITH EXHAUSTIVE SEARCH

Number of bins	Time cost (S)
256	20.8
128	11.4
64	7.5
32	5.9
16	4.5
8	4.4
4	4.3

good solutions much more quickly than other evolutionary algorithms (Eberhart *et al.*, 1998). It is conceptually simple, requires fewer parameters, and is easy to implement (Eberhart *et al.*, 2004).

### The Particle Swarm Optimization (PSO) Algorithm

The PSO is an evolutionary computation technique. It is a population-based search algorithm and is initialized with a population of random solutions, called a particle swarm. Here, one particle indicates a possible matching position in the input image inside the reference image, and is generally randomly produced. A particle swarm consists of a number of particles or “possible solutions” that proceed (fly) through the feasible solution space to explore optimal solutions.

In PSO, the coordinates of each particle represent a possible solution associated with two vectors, the position  $X_i(t)$  and velocity  $V_i(t)$  vectors.  $V_i(t)$  denotes a change of a particle's position. The size of vectors  $X_i(t)$  and  $V_i(t)$  is equal to the problem space dimension  $D$ . Here,  $D$  equals two, since only the translations along the x-axis and y-axis are considered. Assume a swarm consisting of  $M$  particles. The position of the  $i^{\text{th}}$  particle is, in effect, a  $D$ -dimensional vector:

$$X_i = (x_{i1}, x_{i2}, \dots, x_{iD})^T.$$

The velocity of this particle is also a  $D$ -dimensional vector:

$$V_i = (v_{i1}, v_{i2}, \dots, v_{iD})^T$$

where  $i = 1, 2, \dots, M$  is a particle index.  $V_i$  is dynamically adjusted in terms of a particle's own previous best solution,  $pbest_i(t)$ , and the previous best solution of the entire swarm,  $gbest(t)$ . The velocity updates are calculated as a linear combination of the position and velocity vectors according to the following equations (Shi *et al.*, 1998):

$$V_i(t+1) = \omega V_i(t) + c_1 \times \text{rand}() (pbest_i(t) - X_i(t)) + c_2 \times \text{rand}() \times (gbest(t) - X_i(t)) \quad (6)$$

$$X_i(t+1) = X_i(t) + V_i(t+1) \quad (7)$$

where  $t$  is the iteration number,  $X_i(t)$  is the current position of particle  $i$ ,  $\text{rand}()$  is the random number between zero and one,  $c_1$  and  $c_2$  are learning factors,  $pbest_i(t)$  is the best position  $i^{\text{th}}$  particle achieved based on its own experience,  $gbest(t)$  is the best particle position based on the overall swarm experience, and  $pbest_i(t)$  and  $gbest(t)$  are given by the following equations, respectively:

$$pbest_i = \begin{cases} pbest_i; f(X_i) \leq f(pbest_i) \\ X_i; f(X_i) > f(pbest_i) \end{cases} \quad (8)$$

$$\begin{aligned} gbest &\in \{pbest_0, pbest_1, \dots, pbest_m\} \setminus \{gbest\} \\ &= \max (f(pbest_0), f(pbest_1), \dots, f(pbest_m)) \end{aligned}$$

where  $f$  is the objective function,  $m \leq M$ , and  $M$  is the total number of particles in the swarm. In the paper,  $f$  denotes the MI function, and  $\omega$  is an inertia weight that is employed to manipulate the impact of the previous history of velocities on the current velocity. It resolves the tradeoff between the global (wide ranging) and local (nearby) exploration ability of the swarm. A large inertia weight encourages global exploration, while a small one promotes local exploration. A suitable value for  $\omega$  can provide the desired balance between the global and local exploration ability of the swarm and, consequently, improves the effectiveness of the algorithm. Inspired by Shi *et al.* (1998 and 1999), suppose the inertial weight  $\omega$  is a monotonically decreasing function, given  $\omega_{\max} = 0.9$  and  $\omega_{\min} = 0.2$ , and  $T$  is the maximum number of iterations,  $\omega$  is updated as follows (Wachowiak, 2004):

$$\omega(t+1) = \omega(t) + d\omega, \quad d\omega = \frac{(\omega_{\min} - \omega_{\max})}{T}. \quad (9)$$

We refer to Equations 6, 7, 8, and 9 as the Standard PSO.

Like other global optimization algorithms, PSO has the property of being trapped into premature convergence for some optimization problems. Clerc and Kennedy (2002) introduced a constriction factor into PSO to control the convergence properties of the particles. If this constriction factor is included in Equation 6, then:

$$\begin{aligned} V_i(t+1) &= \chi(V_i(t) + c_1 \times \text{rand}() \times (pbest_i(t) - X_i(t)) \\ &\quad + c_2 \times \text{rand}() \times (gbest(t) - X_i(t))) \end{aligned} \quad (10)$$

$$\text{with } \chi = \frac{2k}{|2 - c - \sqrt{c^2 - 4c}|}, \quad c = c_1 + c_2, \quad c > 4, \quad k \in [0, 1].$$

In our experiment, we set  $k = 1.0$ ,  $c_1 = 2.8$ ,  $c_2 = 1.3$  (Wachowiak *et al.*, 2004; Carlisle and Dozier, 2001). This variant is commonly used in many fields and promising in reaching the optimal performance. Here, this approach is named PSO2.

#### A Modified PSO: CRI-PSO Algorithm

One of the methods to satisfy various application purposes, and to prevent premature convergence of the PSO, is to enhance the particle diversity. Some researchers have merged or combined PSO with other evolutionary computation techniques (Lvbjerg *et al.*, 2001; Higashi *et al.*, 2003) to enhance the particle diversity. Van den Bergh (2001) proposed a multi-start PSO, which maintains the historic optimal position of the particle swarm and reinitializes all the particles after having iterated for a certain amount of time in order to improve the swarm diversity and enlarge the searching space. This algorithm can escape from the local minimum and ensure that the search will converge to the global optimization, but it destroys the structure of the current particles with reinitialization, which results in a slowing down of the convergence speed and a great decrease of search accuracy (Li *et al.*, 2004). It is found that reinitialization of particle velocity is a powerful method to avoid the premature convergence of the swarm (Pasupuleti *et al.*, 2006), but how and when to implement reinitialization is important to overcome the drawback of the multi-start PSO.

In the following, we introduce an improved condition for PSO reinitialization (CRI-PSO).

CRI-PSO accepts that each individual is not simply influenced by the best performer among its neighbors. If each particle has avoided premature convergence in the early stages of the search, the capacity for convergence to the global optimum could be enhanced during subsequent stages of the search. Thus, in each iteration in CRI-PSO, if one particle's  $f(pbest)$  (i.e., its historical best fitness function value, i.e., the MI similarity measure value at position  $pbest$ ) does not vary after two continuous iterations, this particle's velocity will be reinitialized. Additionally, the total number of particles to be reinitialized in each iteration is less than a threshold  $N_{\text{predefined}}$  to prevent much more particles from being reinitialized at the later stages of the search. The velocity vector  $V(t+1)$  is updated as follows:

$$\begin{aligned} \text{If } (f(pbest_i(t)) &= f(pbest_i(t-1))) \\ \forall V_i(t+1) &= \text{rand}(V_{\max}, V_{\min}) \\ \text{else } \forall V_i(t+1) &= \chi(V_i(t) + c_1 \times \text{rand}() \times (pbest_i(t) - X_i(t)) \\ &\quad + c_2 \times \text{rand}() \times (gbest(t) - X_i(t))). \end{aligned} \quad (11)$$

In this manner, whether a particle is reinitialized or not is determined by its solution quality, i.e., whether its  $f(pbest)$  value is improved after a certain number of iterations. If the particle is trapped into a local optimum, it would be reinitialized at once. For each time of iteration, some particles with the worst solution quality will be reinitialized. Therefore, they can avoid premature convergence. Particles with better solution quality will update their velocity by the constriction factor. This avoids blind reinitialization for all particles. Thus, with CRI-PSO, the swarm's diversity can be improved and the searching space can be enlarged. In addition, it does not destroy the structure of the current particles. High search accuracy is empirically validated (see Table 5). From Table 5, we can see that the success rate for matching is improved, from 59.8 percent to 76.1 percent for PSO1 and CRI-PSO, respectively.

This approach is different from that proposed by Li *et al.* (2004) at least in two respects. The first is the condition under which reinitialization should be implemented. The condition of reinitialization in Li *et al.* (2004) is that the global historical optimal position  $gbest$  remains continuously unchanged or has changed only a little. In other words, the condition for reinitialization is whether the particle swarm is aggregated heavily. The maximum Euclidean distance between all particles and  $gbest$  were used to express the degree of aggregation of the particle swarm. The reinitialization condition needed in CRI-PSO is based on individual particles. The second difference is who should be reinitialized. In the approach proposed by Li *et al.* (2004), once the condition under which reinitialization occurs is satisfied,  $gbest$  should be kept and some dimensions of all particles' position and velocity vectors in the swarm should be reinitialized according to the mutation probability  $\rho$ . In CRI-PSO, once one particle's  $f(pbest)$  does not vary after two continuous iterations, only this particle's velocity is reinitialized randomly. Its position vector  $X_i$  should not be reinitialized randomly. On the contrary,  $X_i$  should still be adjusted according to Equation 7.

Figure 3 shows the curves of the similarity measure value obtained at  $gbest(f(gbest))$  for the CRI-PSO and the standard PSO along with the times of iteration, respectively. For the standard PSO, it can be seen that a large variation occurred for the similarity measure value before 20 iterations, and an MI of 0.064 was found quickly but no further variation took place in subsequent iterations. This indicates

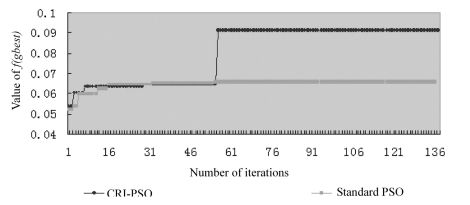


Figure 3. Curves of similarity values at  $g\text{best}(f(g\text{best}))$ .

that the standard PSO method has a strong exploring ability in the earlier iterations, but once it is trapped into a local optimal position, it is difficult to find the global optimal solution. The CRI-PSO found the global best solution,

$MI = 0.091$ , after 54 iterations. From Figure 3, we can find that the modified CRI-PSO method has a stronger ability to find global optimal solutions than the standard PSO. The following additional experiment also verified this conclusion.

## Experiment and Discussions

### Experimental Data

Parts of our test images captured by different sensors are shown in Figure 1 and Figure 4. Test images from several sensors are summarized in Table 3. We have three sets of images to be matched from different sensors: SPOT4 panchromatic (pan) and IRS-C (pan) (Dataset (A)), RadarSAT-1 C and SPOT5 multispectral (Dataset (B)), and SPOT5 (pan) at different dates (Dataset (C)). The RadarSAT-1 C image has a wavelength of 5.6 cm, HH polarization, and was acquired at an angle of incidence of 23.989°.

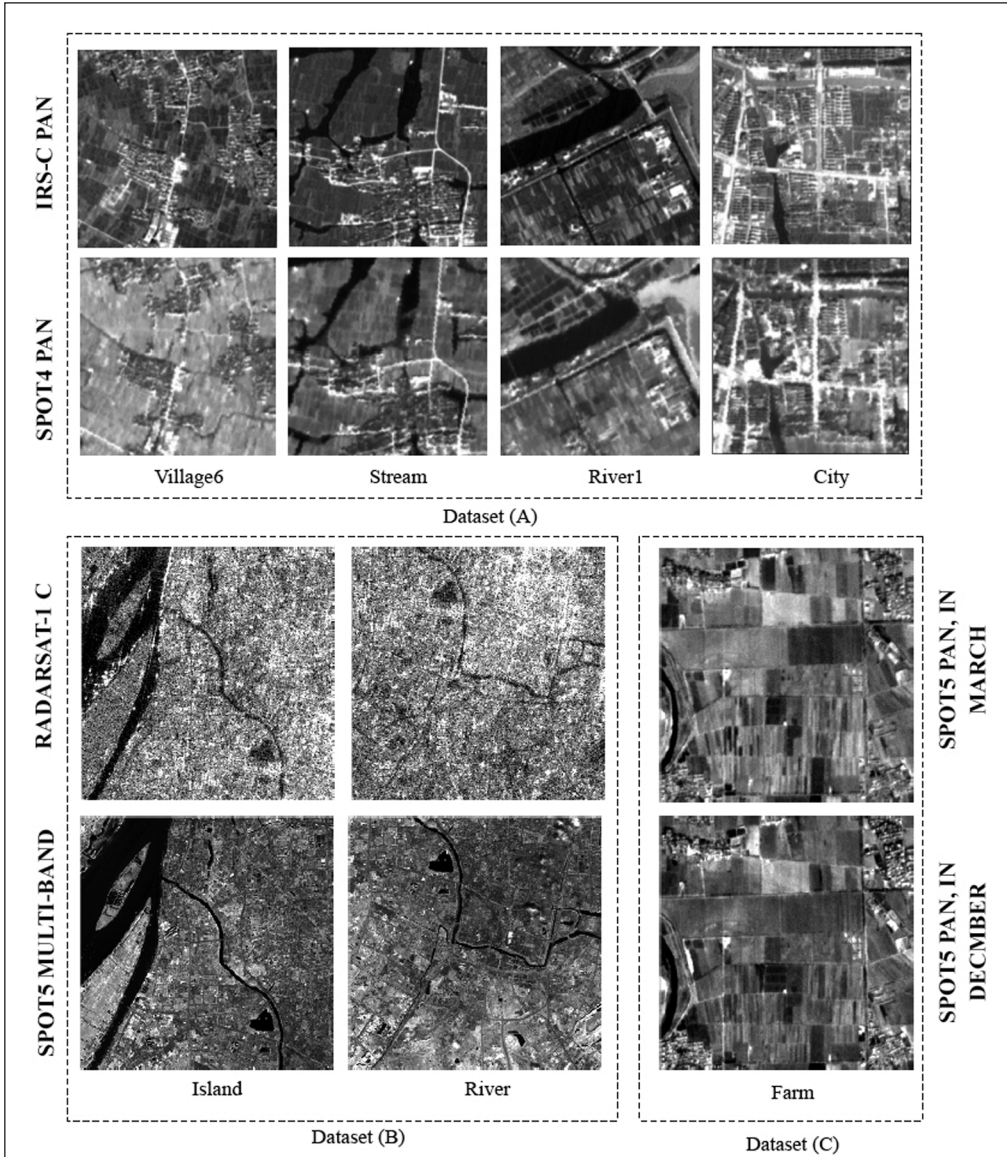


Figure 4. Experimental datasets: Dataset (A): IRS-C pan (above) and SPOT4 pan (below); Dataset (B): RadarSAT-1 C band (above) and SPOT5 multi-spectral (below); and Dataset (C): SPOT5 pan at different dates.

TABLE 3. DIFFERENT SATELLITE SENSORS AND THEIR PROPERTIES

Sensors	SPOT4	IRS-C	SPOT5	RadarSAT-1	SPOT5
Imaging time	Dec. 1999	Jul. 1996	Jul. 2003	Jun. 2003	Dec. 2002; Mar. 2003
Imaging site	Shaoxing, Zhejiang Province, China	Shaoxing, Zhejiang Province, China	Nanjing, Jiangsu Province, China	Nanjing, Jiangsu Province, China	Shaoxing, Zhejiang Province, China
Band Spatial resolution (meters)	Pan 10	Pan 5.8	NIR, R, G 10	C 12.5	Pan 5

All image pairs are  $256 \times 256$  pixels in dimension. In each pair, one image is used as the reference image and the other as the source image for selecting templates for matching. Several template image samples of  $65 \times 65$  pixels were obtained by cropping the source image with an interval of 20 pixels apart from the upper left corner of each template image sample. Thus, 100 template image samples should be derived from a source image. The test areas include flat terrain with farmlands, roads, villages, towns, water areas, or city zones. The reference images and source images are approximately aligned and the pixel size of the image with the lower resolution in a pair is resampled to that of the higher resolution in that pair.

The computer configuration is as follows: CPU: Mobile Intel Pentium M 705; Main Frequency: 1.5GHZ; EMS memory; 512M Programming language: VC++ 6.0.

#### Optimal Choice of Parameters for PSO

In PSO, problem-based tuning of parameters is also a key factor for finding the optimal solution accurately and efficiently. Many empirical values of the parameters for PSO are investigated for different problems. Here, the parameters for PSO are set as follows:

1.  $V_{\max}$ : This determines the largest distance the particle can move in each iteration. In our experiments, the range of a particle's movement is set to the range of the template image moving in the reference image.  $V_{\max} = 256 - 65 = 191$ .
2. Learning factors  $c_1$  and  $c_2$ : These are set to  $c_1 = c_2 = 2$  for the standard PSO, according to Eberhart and Shi (2001) and Clerc (1999).
3. The range of the position of the particle  $X_{\min}$  and  $X_{\max}$ : These refer to the range of the solution determined by the optimal problem.  $X_{\min} = 0$  and  $X_{\max} = 191$ .
4. Dimensions of the particle: They are determined by the optimal problem. The dimensions of the particle are set to 2 because the matching is only done in 2D.
5. Stopping criterion: The stopping criterion used in the experiment is the iteration that is regarded as convergence when  $f(gbest)$  has not been improved after iteration for a given number of times. The stopping criterion is set to 30 based on the test shown in Figure 5, in which we can see that the success rate increases as the increase of the given number of consecutive iterations, and the time cost is the same. For example, when the stopping criterion is set to 30, the success rate is 93 percent, and time cost is 0.64(s). Whereas when the stopping criterion is set to 100, the success rate is 95 percent, and time cost is 1.32 (s). We find that the success rate is increased slightly as a whole, but the time cost is increased greatly. So in the paper's experiments, the stopping criterion is set to 30 except the experiment in Table 4.

The test data used in Figure 5 are those Stream image pairs, and 100 template image samples are used. The CRI-PSO algorithm is used and the size of swarm population is 90.

6. Size of swarm population: The population size selected is problem-dependent. Sizes of 20 to 50 are most common. In some situations, large population sizes may be used to

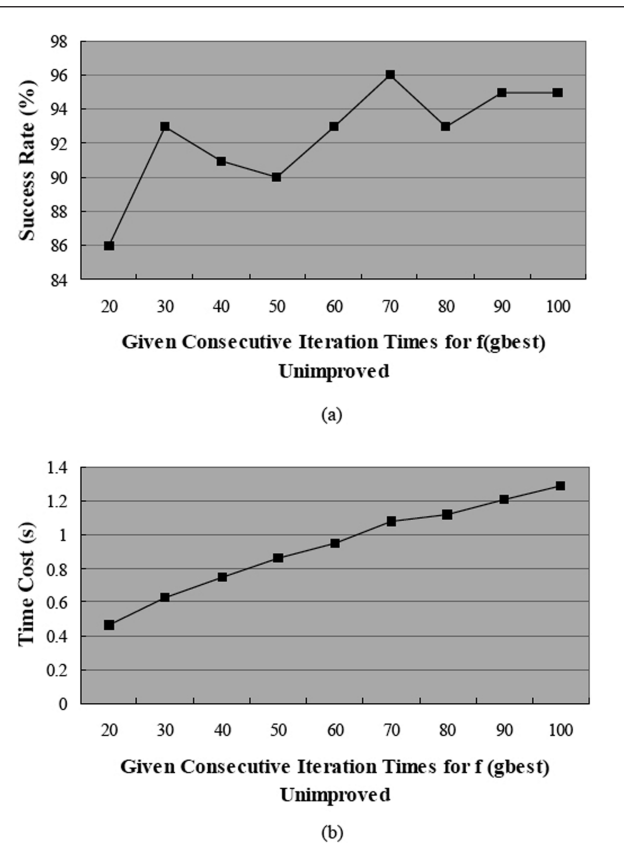


Figure 5. Variance of matching performance along with the increase of the number of consecutive iterations during which  $f(gbest)$  is invariant:  
(a) success rate, and (b) time cost

TABLE 4. THE SUCCESS RATE AND TIME COST FOR MATCHING WITH DIFFERENT SIZE OF SWARM POPULATION

Size of swarm population	Time cost (S)	Total iteration times	Success rate (%)
100	1.13	116	77.8
90	0.89	113	72.4
80	0.71	115	71.1
70	0.71	115	66.8
60	0.55	118	67.7
50	0.54	117	69.0
40	0.39	116	59.3
30	0.28	120	53.3
20	0.18	107	43.2

adapt to different requirements. The experiment in the paper also illustrates this. The relationship between the size of the swarm population and the success rate and computation is shown in Table 4. The test data used is the Stream image pair. The standard PSO is used. Here, the stopping criterion is set to 80. From it, we can see that the success rate increases as the increase of the size of swarm population as a whole, and the time cost is the same. The size of the swarm population from 50 to 100 is all acceptable. The larger the size of swarm population is, the more reliable result can be obtained. Here, it is set to 90 in order to adapt the matches for different types of images processed.

## Experimental Results

### Matching Results of Different PSO Variants

The PSO variants used for comparison include the following methods:

1. PSO1: Standard PSO (Shi *et al.*, 1998). Equations 6, 7, 8, and 9 are referred to as the Standard PSO. Suppose  $c_1 = c_2 = 2$  (Eberhart and Shi, 2001; Clerc, 1999). Linearly decreasing inertia weight  $\omega$  is set from 0.9 to 0.2, according to Shi *et al.* (1998 and 1999) and Wachowiak *et al.* (2004). Suppose  $T = 120$ , according to empirical experiment.
2. PSO2: PSO with constriction factors. A constriction factor is included in the PSO to control the convergence properties of the particles (Equation 10). The initial particle position is produced randomly. Suppose  $k = 1.0$ ,  $c_1 = 2.8$ ,  $c_2 = 1.3$  (Wachowiak *et al.*, 2004; Carlisle and Dozier, 2001).
3. PSO3: PSO with constriction factors and initial particle position distributed uniformly. The parameters are the same as in PSO2.
4. PSO4: Multi start PSO. The parameters are the same as in PSO1.
5. PSO5: CRI-PSO proposed in the paper. In the CRI-PSO,  $c_1$  and  $c_2$  are determined by following equations in terms of Ratnaweera *et al.* (2004):

$$c_1 = (c_{1f} - c_{1i}) \frac{iter}{T} + c_{1i} \quad (12)$$

$$c_2 = (c_{2f} - c_{2i}) \frac{iter}{T} + c_{2i} \quad (13)$$

where  $c_{1f}$  and  $c_{2f}$  are acceleration coefficients in the final iteration;  $c_{1i}$  and  $c_{2i}$  are acceleration coefficients in the initial iteration.  $T$  is the maximum number of iterations;  $iter$  is the current times of iterations. Generally, set  $c_{1i} = 2.5$ ,  $c_{1f} = 0.5$ ,  $c_{2i} = 0.5$ , and  $c_{2f} = 2.5$ . The value of acceleration coefficient  $c_1$  decreases from 2.5 to 0.5 and  $c_2$  increases from 0.5 to 2.5. Set  $N = 45$  validated by empirical test. Other parameters are the same as in PSO1.

Comparison results are shown in Figure 6 and Figure 7. The test data we used is the Stream image pair. The number of template images is 100. The success rate of the method, in which MI calculated with 16 bins and an exhaustive searching strategy are used, is 100 percent (exhaustive searching means all possible matching positions are searched out and compared with each other, and the most optimal solution is found; this search strategy is very slow in practice, although it produces the highest match rate). It is found that PSO1, PSO2, and PSO3 have lower success rates in our applications because the similarity measure distribution is non-convex and irregular, and it has many local maxima (shown in Figure 2). PSO4 has better performance than the three previously mentioned PSO variants. Clearly, reinitialization is efficient for particles to escape from local minima. PSO5 (i.e., CRI-PSO), the method suggested here, outperforms all the other methods. In Figure 7, it can be seen that the computation cost of PSO5 is slower slightly than PSO1, but it is faster than other three methods.

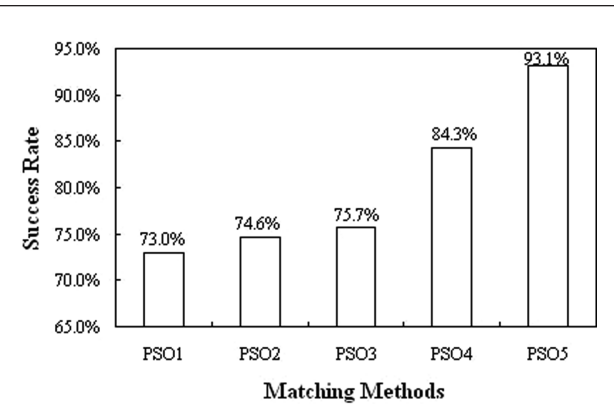


Figure 6. Success rate of different PSO variants:  
 PSO1: Standard PSO; PSO2: PSO with constriction factors; PSO3: PSO2 with initial particle position distributed uniformly; PSO4: Multi start PSO; and PSO5: CRI-PSO proposed in the paper.

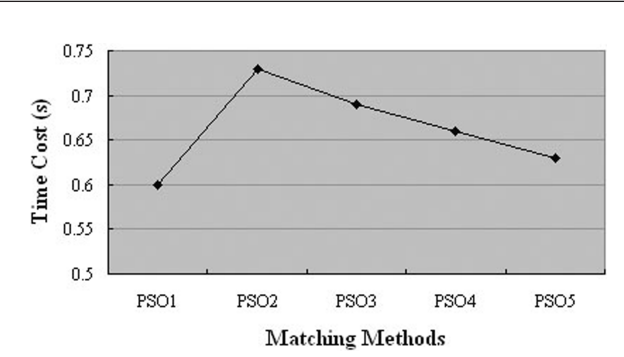


Figure 7. Computation requirements of different PSO variants.

### Matching Experiment using Different Scenes in SPOT4 Pan and IRS-C Pan Datasets

Different image pairs (shown in Figure 1 and Figure 4) were used in this experiment in order to test the stability and reliability of the proposed method. Performances were compared among the MI-based methods and NCC (Table 5). It is found that image matching with 16 bins for the MI is very robust, because it achieved a high success rate even though the matching images contain contrast reversals and more self-similar patterns, such as the Village6 image pair and the Farmland pair. The success rate of NCC is much lower for the Village6 and Farmland image pairs.

The CRI-PSO outperformed the Standard PSO and NCC in terms of the success rate of matching. The computation time required by CRI-PSO is similar to that of the Standard PSO, and about six times faster than that of the NCC. Compared with the MI-based method with 16 bins and the exhaustive searching strategy, the CRI-PSO has a relatively lower success rate (about 10 percent lower than that of the exhaustive search method).

### Matching Experiments using Multi-sensor Dataset

In addition to the SPOT4 and IRS-C dataset, datasets using RadarSAT-1 C band and SPOT5, and SPOT5 on different dates are also tested in our experiment. The matching performance is given in Table 6.

TABLE 5. COMPARISONS OF MATCHING RESULTS OF FOUR METHODS

Images used to trail	Number of template images	16-bin MI (Exhaustive searching)		16-bin MI Standard PSO (PSO1)		16-bin MI CRI-PSO (PSO5)		NCC (Exhaustive searching)	
		Success rate (%)	Time cost (s)	Success rate (%)	Time cost (s)	Success rate (%)	Time cost (s)	Success rate (%)	Time cost (s)
Town	100	95	4.52	55	0.64	81	0.77	85	4.11
Farmland	100	80	4.52	58	0.68	75	0.72	28	4.58
River1	100	89	4.52	73	0.62	83	0.75	63	4.48
Village	100	86	4.51	56	0.65	72	0.64	61	4.49
City	100	92	4.50	65	0.81	84	0.79	65	3.98
Village6	100	66	4.51	39	0.73	45	0.73	10	4.19
Stream	100	100	4.51	73	0.60	93	0.63	82	4.46
	Mean	86.7	4.51	59.8	0.67	76.1	0.72	56.3	4.33

TABLE 6. COMPARISONS OF MATCHING RESULTS FOR DIFFERENT DATASETS

Dataset	Number of template images	16-bin MI (Exhaustive searching)		16-bin MI Standard PSO (PSO1)		16-bin MI CRI-PSO (PSO5)		NCC (Exhaustive searching)	
		Success rate (%)	Time cost (s)	Success rate (%)	Time cost (s)	Success rate (%)	Time cost (s)	Success rate (%)	Time cost (s)
SPOT4 pan and IRS-C pan	700	86.7	4.51	59.8	0.67	76.1	0.72	56.3	4.33
RadarSAT-1 C and SPOT5 multi-band	600	62.1	4.27	41.0	0.63	51.8	0.70	19.8	4.21
SPOT5pan at different dates	400	100.0	4.31	78.0	0.62	94.1	0.69	97.5	4.19

From the experimental result, it is observed that the success rate of the MI with the exhaustive searching method is much higher than that of NCC, whether the matching images are captured by radar or the optical sensors. However, the time consumed by the MI methods is appreciably longer than that of NCC. For the test images from radar and optical sensors, e.g., the RadarSAT-1 and SPOT5 dataset, the success rate of MI is much higher than that of NCC. For images acquired from optical sensors, e.g., the SPOT4 and IRS-C dataset, or the SPOT5 on different dates, the success rate of MI is also higher than that of NCC. Because the time and season of the images captured by these two sensors are different, and there is a change of the landscapes, the performance of the NCC is poor, and the MI measure still maintains good performance. This illustrates that the MI is robust, reliable, and suitable for matching satellite images acquired by multiple sensors with similar resolution, such as SPOT4 pan (10 meter) and IRS-C pan (5.8 meter), and RadarSAT-1 C (12.5 meter) and SPOT5 multi-spectral (10 meter).

For the CRI-PSO proposed in the paper, its time cost for matching is improved greatly compared to that of MI with exhaustive searching and NCC. Its success rate is much better than that of NCC, but the success rate is slightly reduced compared to that of MI with exhaustive searching. From the trade-off between success rate and time cost, we can see that CRI-PSO is a promising optimizing method for fast image matching.

SIFT method (Lowe, 2004) is also tested using RadarSAT-1 C and SPOT5 images. The matching is almost all failure. The matching results of different scene for RadarSAT-1 C and SPOT5 images by CRI-PSO are shown in Figure 8 and Figure 9.

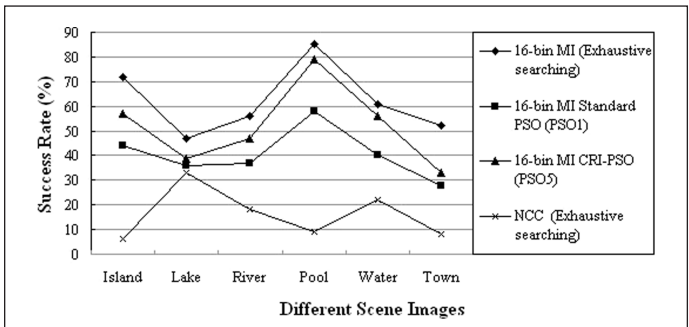


Figure 8. Success rate of various methods among different scenes of RadarSAT-1 C and SPOT5.

From the test results, we can see that the match rates between the optical sensors are greater than those between optical and radar sensors. Therefore, to make the mutual information criterion more useful for the application of SAR image registration, some efforts should be made to further improve the robustness of MI, for example, reducing speckle in radar images and improving interpolation algorithms for suppressing interpolation artifacts.

## Conclusions

Cross-correlation based algorithms are often used in template matching in practice, but they are sensitive to nonlinear changes of the image intensity and random noise. Here, we

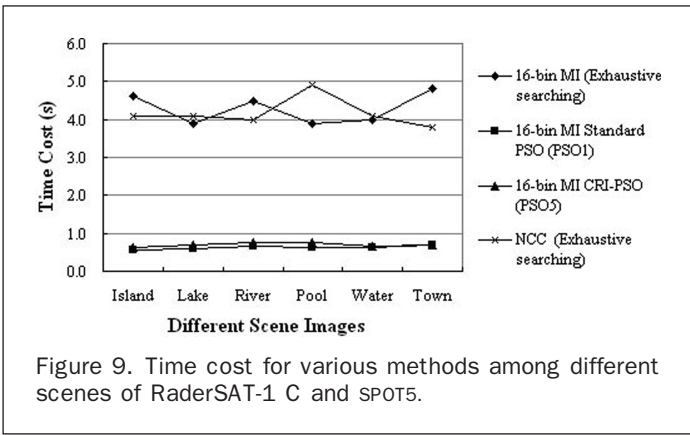


Figure 9. Time cost for various methods among different scenes of RaderSAT-1 C and SPOT5.

introduce the normalized mutual information (MI) to overcome the drawback of the cross-correlation algorithm. The validity of MI is checked by experiments using multi-sensor images. Because the MI-based matching algorithms are time consuming, a global optimal method is needed to accelerate the match process. Particle swarm optimization (PSO) methods can be used to accelerate the matching process. We proposed a modified PSO, named CRI-PSO, to improve convergence. We carried out experiments with various PSO in MI-based template matching. The experimental results show that the CRI-PSO can not only speed up the matching but also improve the match rates when compared to the standard PSO and NCC methods. Our results indicate that the proposed method is promising and viable for template matching. How to enhance the calculation efficiency for the MI-based template matching needs further research. There is still room to improve the match rates while overcoming the premature convergence problem of the PSO methods. For radar image matching, means to reduce speckle noise and suppress interpolation artifacts also need further study. Finally, it is desirable to develop additional measures to determine genuinely correct matching, i.e., how to discard mismatches from those matches with high similarity.

## Acknowledgments

This research is supported by the State Key Laboratory of Remote Sensing Science, a grant from National Nature Science Foundation of China (No. 40771137), a grant from the National 863 Program (2008AA12Z106), partially supported by 2006103269 NNSFC, and a one hundredth talent grant from the Chinese Academy of Sciences.

The authors wish to thank three anonymous referees and editors for providing many constructive suggestions that greatly improved the quality on an earlier version of this paper.

## References

- Alrashidi, M.R., and M.E. El-Hawary, 2006. A survey of particle swarm optimization applications in power system operations, *Electric Power Components and Systems*, 34:1349–1357.
- An, R., H.L. Wang, and X.Z. Feng, 2005. Investigation of image corner features matching algorithm based on heuristic local geometric restriction strategy, *Proceedings of the SPIE International Conference on Space Information Technology*, 19–20 November, Wuhan, China, pp.59852R1-6.
- Angeline, P.J., 1998. Evolutionary optimization versus particle swarm optimization: Philosophy and performance differences, *Evolutionary Programming*, 7:601–610.
- Brown, L.G., 1992. A survey of image registration techniques, *ACM Computing Surveys*, 24(4):325–376.
- Carlisle, A., and G. Dozier, 2001. An off-the-shelf PSO, *Proceedings of the Workshop on Particle Swarm Optimization*, Indianapolis, Indiana: Purdue School of Engineering and Technology, IUPUI.
- Chen, H.M., M.K. Arora, and P.K. Varshney, 2003. Mutual information-based image registration for remote sensing data, *International Journal of Remote Sensing*, 24(18):3701–3706.
- Chen, H.M., P.K. Varshney, and M.K. Arora, 2003. Performance of mutual information similarity measure for registration of multitemporal remote sensing images, *IEEE Transactions on Geoscience and Remote Sensing*, 41(11):2445–2454.
- Choi, M.S., and W.Y. Kim, 2002. A novel two stage template matching method for rotation and illumination invariance, *Pattern Recognition*, 35:119–129.
- Clerc, M., and J. Kennedy, 2002. The particle swarm - Explosion, stability, and convergence in a multidimensional complex space, *IEEE Transactions on Evolutionary Computation*, 6:58–73.
- Clerc, M., 1999. The swarm and the queen: towards a deterministic and adaptive particle swarm Optimization, *Proceedings of the IEEE Congress on Evolutionary Computation (CEC 1999)*, pp. 1951–1957.
- Cole-Rhodes, A.A., L.J. Kisha, L.M. Jacqueline, and Z. Ilya, 2003. Multiresolution registration of remote sensing imagery by optimization of mutual information using a stochastic gradient, *IEEE Transactions on Image Processing*, 12(12):1495–1511.
- Cover, T.M., and J.A. Thomas, 1991. *Elements of Information Theory*, New York: John Wiley & Sons.
- Du, F., W.K. Shi, L. Z. Chen, Y. Deng, and Z.F. Zhu, 2005. Infrared image segmentation with 2-D maximum entropy method based on particle swarm optimization (PSO), *Pattern Recognition Letters*, 26:597–603.
- Eberhart, R.C., and Y.H. Shi, 2004. Guest editorial special issue on particle swarm optimization, *IEEE Transactions on Evolutionary Computation*, 8(3):201–203.
- Eberhart, R.C., and Y.H. Shi, 1998. Comparison between genetic algorithms and particle swarm optimization, *Proceedings of the 7<sup>th</sup> International Conference on Evolutionary Programming*, 1447, pp.611–616.
- Eberhart, R.C., and Y.H. Shi, 2001. Particle swarm optimization: Developments, applications and resources, *Proceedings of the IEEE Congress on Evolutionary Computation (CEC 2001)*, Seoul, Korea.
- Gong, P., E.F. LeDrew, and J.R. Miller, 1992. Registration noise reduction in difference images for change detection, *International Journal of Remote Sensing*, 13(4):773–779.
- Hu, X.H., Y.H., Shi, and R. Eberhart, 2004. Recent advances in particle swarm, *Proceedings of the 2004 Congress on Evolutionary Computation*, 1, pp.90–97.
- Higashi, N., and H. Iba, 2003. Particle swarm optimization with Gaussian mutation, *Proceedings of the 2003 Swarm Intelligence Symposium, SIS Apos:03*, IEEE, 24–26, pp.72 - 79.
- Ingla, J., 2002. Similarity measures for multisensor remote sensing images, *Proceedings of IGARSS*, Toronto, Canada (Piscataway, New Jersey: IEEE Geoscience and Remote Sensing Society), unpaginated CD ROM.
- Johnson, K., A.C. Rhodes, I. Zavorin, and J. Lemoigne, 2001. Mutual information as a similarity measure for remote sensing image registration, *Proceedings of the SPIE*, 4383, pp.51–61.
- Josien, P.W.P., J.B. Antoine Maintz, and M.A. Viergever, 2003. Mutual information based registration of medical images: A survey, *IEEE Transactions on Medical Imaging*, 22(8):986–1004.
- Kennedy, J., and R. Eberhart, 1995. Particle swarm optimization, *Proceedings of the IEEE International Conference on Neural Networks*, 4, pp.1942–1948.
- Kern, J.P., and S.P. Marios, 2007. Robust multi spectral image registration using mutual-information models, *IEEE Transactions on Geoscience and Remote Sensing*, 45(5):1494–1505.

- Knops, Z.F., and J.B.A. Maintz, 2006. Normalized mutual information based registration using k-means clustering and shading correction, *Medical Image Analysis*, 10:432–439.
- Li, N., Y.-Q. Qin, D.-B. Sun, and T. Zou, 2004. Particle swarm optimization with mutation operator, *Proceedings of the Third International Conference on Machine Learning and Cybernetics*, 26–29 August, Shanghai, China.
- Liu, D., P. Gong, M. Kelly, and Q. Guo, 2006. Automatic registration of airborne images by combining area-based methods with local transformation models, *Photogrammetric Engineering & Remote Sensing*, 72(9):1049–1059.
- Lo, C.H., 2003. *Medical Image Registration by Maximization of Mutual Information*, Ph.D. dissertation, Kent State University.
- Lowe, D.G., 2004. Distinctive image features from scale-invariant keypoints, *International Journal of Computer Vision*, 60(2):91–110.
- Lvbjerg, M., T.K. Rasmussen, and T. Krink, 2001. Hybrid particle swarm optimizer with breeding and subpopulations, *Proceedings of the Genetic and Evolutionary Computation Conference (GECCO-2001)*, Morgan Kaufmann, pp. 469–476.
- Maes, F., A. Collignon, D. Vandermeulen, G. Marchal, and P. Suetens, 1997. Multimodality image registration by maximization of mutual information, *IEEE Transactions on Medical Imaging*, 16:187–198.
- Maitra, M., and A. Chatterjee, 2007. A hybrid cooperative - Comprehensive learning based PSO algorithm for image segmentation using multilevel thresholding, *Expert Systems with Applications*, doi: 10.1016/j.eswa.2007.01.002
- Mendes, R., J. Kennedy, and J. Neves, 2004. The fully informed particle swarm: Simpler, maybe better, *IEEE Transactions on Evolutionary Computation*, 8(3):204–210.
- Oh, Y.S., D.G. Sim, R.H. Park, R.C. Kim, S.U. Lee, and I.C. Kim, 2006. Absolute position estimation using IRS satellite images, *ISPRS Journal of Photogrammetry and Remote Sensing*, 60:256–268.
- Pasupuleti, S., and R. Battiti, 2006. The gregarious particle swarm optimizer (G-PSO), *Proceedings of the 8<sup>th</sup> Annual Conference on Genetic and Evolutionary Computation*, Seattle, Washington, Session on ant colony optimization and swarm intelligence, pp. 67–74.
- Pluim, J.P.W., J.B.A. Maintz, and M.A. Viergever, 2001. Mutual information matching in multiresolution contexts, *Image and Vision Computing*, 19:45–52.
- Ratnaweera, A., S.K. Halgamure, and H.C. Watson, 2004. Self-organizing hierarchical particle swarm optimizer with time-varying acceleration coefficients, *IEEE Transactions on Evolutionary Computation*, 8:240–255.
- Shi, Y., and R.C. Eberhart, 1998. A modified particle swarm optimizer, *Proceedings of the IEEE Congress on Evolutionary Computation*, Piscataway, New Jersey, pp.69–73.
- Shi, Y., and R.C. Eberhart, 1998. Parameter selection in particle swarm optimization, *Proceedings of the 7<sup>th</sup> International Conference on Evolutionary Programming VII*, Springer-Verlag, New York, LNCS Vol. 1447, pp.591–600.
- Shi, Y., and R.C. Eberhart, 1999. Empirical study of particle swarm optimization, *Proceedings of the IEEE International Congress Evolutionary Computation*, Vol. 3, pp. 101–106.
- Sim, D.G., S.Y. Jeong, D.H. Lee, R.H. Park, R.C. Kim, S.U. Lee, and I.C. Kim, 1999a. Hybrid estimation of navigation parameters for aerial image sequence, *IEEE Transactions on Image Processing*, 8(3):429–435.
- Sim, D.G., O.K. Kwon, and R.H. Park, 1999b. Object matching algorithm using robust Hausdorff distance measures, *IEEE Transactions on Image Processing*, 8(3):425–429.
- Studholme, C., D.L.G. Hill, and D.J. Hawkes, 1999. An overlap invariant entropy measure of 3D medical image alignment, *Pattern Recognition*, 32(1):71–86.
- Van den Bergh, F., 2001. *An Analysis of Particle Swarm Optimizers*, Ph.D. dissertation, Department of Computer Science, University of Pretoria, South Africa.
- Viola, P., and W. Wells, 1995, Alignment by maximization of mutual information, *Proceedings of the 5<sup>th</sup> International Conference on Computer Vision*, 20–23 June, Cambridge, (Los Almitos, California: IEEE Computer Society Press), pp.6–23.
- Wachowiak, M.P., R. Smolíková, Y.F. Zheng, J.M. Zurada, and A.S. Elmaghhraby, 2004. An approach to multimodal biomedical image registration utilizing particle swarm optimization, *IEEE Transactions on Evolutionary Computation*, 8(3):289–301.
- Xu, P., and D.Z. Yao, 2007. A study on medical image registration by mutual information with pyramid data structure, *Computers in Biology and Medicine*, 37:320–327.
- Yin, P.Y., 2006. Particle swarm optimization for point pattern matching, *Journal of Visual Communication and Image Representation*, 17:143–162.
- Zahara, E., Z. Shu-Kai, S. Fan, and D.M. Tsai, 2005. Optimal multi-thresholding using a hybrid optimization approach, *Pattern Recognition Letters*, 26:1082–1095.
- Zitova, B., and J. Flusser, 2003. Image registration methods: A survey, *Image and Vision Computing*, 21:977–1000.

(Received 27 January 2008; accepted 03 March 2009; final version: 15 July 2009)